

Observation of Odd-Parity Superconductivity with the Geshkenbein-Larkin-Barone Composite Rings

Xiaoying Xu^{1,*}, Yufan Li^{1,2,†} and C. L. Chien^{1,3,‡}

¹*William H. Miller III Department of Physics and Astronomy, Johns Hopkins University, Baltimore, Maryland 21218, USA*

²*Department of Physics, The Chinese University of Hong Kong, Shatin, Hong Kong SAR, China*

³*Department of Physics, National Taiwan University, Taipei 10617, Taiwan*



(Received 25 January 2023; revised 25 November 2023; accepted 19 December 2023; published 29 January 2024)

Phase-sensitive measurements on a composite ring made of a superconductor of interest connected by a known singlet s -wave superconductor can unambiguously determine its pairing symmetry. In composite rings with epitaxial β -Bi₂Pd and s -wave Nb, we have observed half-integer-quantum flux when Nb is connected to the opposite crystalline ends of β -Bi₂Pd and integer-quantum flux when Nb is connected to the same crystalline ends of β -Bi₂Pd. With ascending temperature, the half-integer-flux quantization transits to integer-flux quantization, before the eventual loss of phase coherence. These findings point to odd-parity pairing symmetry in superconducting β -Bi₂Pd.

DOI: [10.1103/PhysRevLett.132.056001](https://doi.org/10.1103/PhysRevLett.132.056001)

Superconductivity is the result of condensation of Cooper pairs, where the pairing of two electrons can form either spin singlet with spin 0 or spin triplet with spin 1. To satisfy Fermi statistics, the spatial part of the pair's wave function must be of even parity for spin-singlet and of odd parity for spin-triplet pairing states. The known superconductors (SCs) are overwhelmingly singlet pairing, including the conventional s -wave SCs and the high- T_c d -wave cuprates. The very rare triplet pairing state has only been confirmed in ³He superfluid [1]. The decades-long quest of searching for intrinsic triplet SCs is currently met with renewed interest as it has been shown that triplet pairing states generally lead to topological superconductivity, essential for realizing Majorana fermions with non-Abelian braiding statistics that facilitates noise-resilient topological quantum computing [2–4].

By the nature of their pairing states, one can decisively distinguish between singlet and triplet SCs by the parity symmetry of its wave function via phase-sensitive experiments [5,6]. It was first proposed by Geshkenbein, Larkin, and Barone (GLB) that a signature half-quantum flux (HQF) can be observed in a composite ring structure, consisting of a triplet p -wave SC connected by a singlet s -wave SC at the opposite ends [5], as depicted in Fig. 1(a). This sign reversal is realized at the two crystalline ends of a triplet SC, generating a π phase shift that leads to fluxoid quantization of half-integer-quantum numbers; $\Phi' = (n + 1/2)\Phi_0$, where Φ_0 is the flux quantum and n is an integer. This is in stark contrast with the ordinary fluxoid quantization with integer-flux quanta of $n\Phi_0$, well established in singlet SCs with even parity $\Delta_k = \Delta_{-k}$.

The first experimental demonstrations of the phase-sensitive methods are in fact a variant of the GLB proposal to reveal the d -wave pairing symmetry in high- T_c

cuprates [7]. Two orthogonally oriented crystal planes of a single crystal YBa₂Cu₃O₇ are connected with a Pb thin film, constituting a corner junction geometry [8,9]. The sign change of the gap function under 90° rotation results in a π phase shift in the Josephson current-phase relation, thus revealing the $d_{x^2-y^2}$ gap structure.

The GLB experiment, in its original design and for the proposed purpose of detecting odd-parity symmetry, was carried out in a Sr₂RuO₄-Au_{0.5}In_{0.5} superconducting quantum interference device (SQUID) to examine the proposed triplet p -wave pairing of Sr₂RuO₄ [10]. In all the aforementioned studies, the samples of interest are bulk single crystals. An inherent challenge with this approach is rooted in the small value of the flux quantum Φ_0 , approximately 20.7 G (μm)². The large sizes of devices when involving bulk specimen, generally on the 100 μm scale, lead to small flux quantization periods in terms of magnetic field on the order of milligauss [8,10]. Extrapolation to identify the zero magnetic field is required for establishing the HQF; this inevitably leaves room for ambiguity [6,11].

We instead employ a planar composite ring structure, composed of thin films of epitaxial β -Bi₂Pd, an odd-parity p -wave SC candidate [12–14], and Nb, an s -wave SC. The thin film specimen has the advantage of allowing the device to be defined by electron-beam (e -beam) lithography. In this study, we fabricated micrometer-sized composite ring devices with the Φ_0 period on the order of 10 Oe in terms of magnetic field. The presence of HQF can be straight forwardly determined from the Little-Parks effect [14,15]. The result shows clear-cut evidence for odd-parity pairing in β -Bi₂Pd. Indeed, by resolving the parity symmetry of the superconducting gap, the composite ring structure can unequivocally reveal the

pairing state of any superconductors. We show that the HQF can be achieved on demand, requiring only appropriate design geometry. The accessible HQF readily integrable with 2D lithography technique opens the door for applications of zero-field flux qubits [14].

We first synthesized epitaxial (001) β -Bi₂Pd films on (001) SrTiO₃ substrates with magnetron sputtering, exploiting the fact that the *ab* plane of β -Bi₂Pd with a tetragonal lattice with $a = b = 3.36$ Å and $c = 12.98$ Å can be epitaxially grown on the (001) SrTiO₃ surface [13,16]. The x-ray diffraction pole-figure measurements of the epitaxial films establishes the epitaxial relationship of [100] β -Bi₂Pd||[100] SrTiO₃; see details in the Supplemental Material [17]. Composite ring devices are patterned by *e*-beam lithography to the submicrometer level, consisting of a segment of epitaxial β -Bi₂Pd and the remainder of polycrystalline Nb. We explored two classes of geometries. The first geometry is the original GLB proposal [5]. A typical device is shown in Fig. 1(e) as the scanning electron microscopic image of device GLB-A, where a straight segment of epitaxial β -Bi₂Pd is connected by Nb at the *opposite* ends. HQF is expected for the odd-parity pairing state in this geometry. In the second geometry, the *same* side of a crystal plane face of β -Bi₂Pd is connected by Nb, as the device SS-B shown in Fig. 1(f). Conventional integer-quantum flux (IQF) is expected for this geometry, regardless of the pairing state. The temperature dependence of a typical ring device shows two sharp transitions at about 3.4 and 8.0 K due to the superconducting transitions of β -Bi₂Pd and Nb, respectively, as shown in Fig. 1(g). Measures are taken to minimize the lateral overlap between β -Bi₂Pd and Nb, so that the contact is made primarily at the sidewalls, described in detail in the Supplemental Material [17].

The Little-Parks effect reveals the oscillation of the superconducting critical temperature T_c as a function of the applied magnetic field threading through the ring, reflecting the periodic variation of the free energy as a result of fluxoid quantization [19]. Experimentally, one observes the oscillation of the resistance of the ring at a fixed temperature below but close to T_c . For the conventional integer-flux quantization, i.e., $\Phi' = n\Phi_0$, the resistance minima occur at integer-quantum numbers, as shown in Fig. 1(d). For HQF, the resistance minima occurs at half-integer-quantum numbers. To avoid artifacts such as trapped vortex, the sample is always cooled down in zero field from 10 K before each measurement. The result is always confirmed by sweeping the field in both directions. The Little-Parks effect of normalized resistance as a function of perpendicularly applied magnetic field in GLB-A at 2.7 K is demonstrated in Fig. 2(a). The measured oscillation period of 4.25 Oe is consistent with the estimated period of about 3.10 Oe from the intended dimension of 4.2×1.6 μm². A small deviation may originate from the flux diversion known for reducing the effective pickup area of SQUID devices with thick

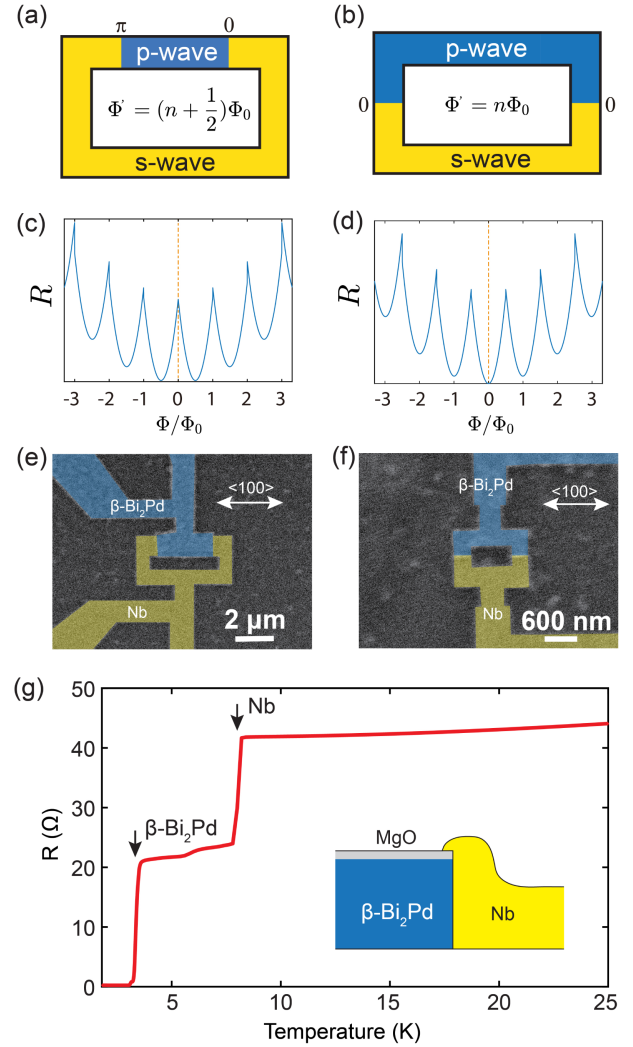


FIG. 1. Two types of triplet and singlet composite ring structures of GLB and SS devices. (a) Schematic and (e) actual GLB ring of a triplet superconductor β -Bi₂Pd with the opposite sides connected at the two ends with *s*-wave Nb exhibits resistance minima only at half-flux quanta, $(n + 1/2)\Phi_0$, as depicted in (c). (b) Schematic and (f) actual SS ring of a triplet superconductor β -Bi₂Pd with the same side connected at two ends with *s*-wave Nb exhibits resistance minima at integer-flux quanta of $n\Phi_0$, as depicted in (d). In both cases, β -Bi₂Pd is an epitaxial layer 70 nm thick oriented laterally along the [100] direction. (g) A representative resistance versus temperature curve of the composite ring device showing the T_c of β -Bi₂Pd and Nb. The inset shows a schematic drawing of the cross section of the β -Bi₂Pd-Nb junction.

walls [20]. For the Little-Parks effect, an aperiodic background originating from, among others, a slight field misalignment [21] and device geometry [22] generally appears with the Φ_0 -periodic oscillations. After the curved background is removed from the raw data in the upper panel, pure Little-Parks oscillation is plotted in the lower panel, which shows the resistance minima at fields corresponding to half-integer flux of $\Phi = (n + 1/2)\Phi_0$.

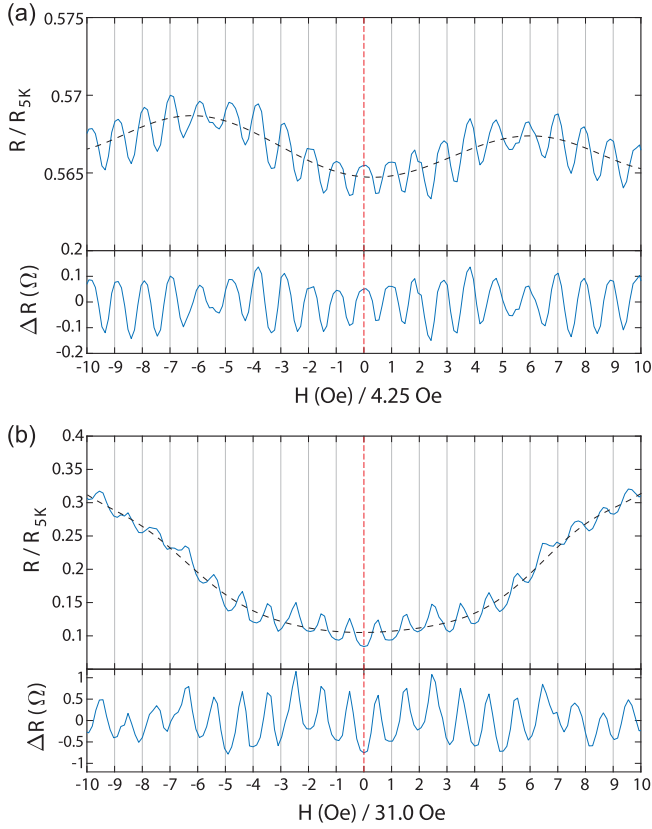


FIG. 2. The Little-Parks effect of GLB-A and SS-B composite rings. Normalized resistance (upper panel) including the background as the dashed curve and the relative resistance (lower panel) with the background removed of (a) GLB-A ($4.2 \times 1.6 \mu\text{m}^2$) showing resistance minima at the half-integer flux quanta $(n + 1/2)\Phi_0$, obtained at 2.7 K, and (b) SS-B ($1.1 \times 0.7 \mu\text{m}^2$) showing resistance minima at the integer-flux quanta $n\Phi_0$, obtained at 3.2 K. The x axes indicate the magnetic field applied perpendicular to the ring area in units 4.25 and 31.0 Oe, respectively, dictated by the ring size, reflecting flux quanta. Grid lines mark integer quanta.

The determination of the zero-field position is straightforward because of the substantial field values of several to several tens of oersted, and that can be further aided by multiple features of the Little-Parks oscillations, such as the symmetry of the curved background, and the symmetrical glitches near $\pm 5.5\Phi_0$. The observation of HQF conclusively shows that $\beta\text{-Bi}_2\text{Pd}$ is an odd-parity SC.

In contrast, the SS-B device demonstrates only the ordinary IQF, as would be expected for any doubly connected superconducting devices. The Little-Parks effect shows an oscillation period of 31.0 Oe, in close agreement with the 27.0 Oe as expected from the ring size of $1.1 \times 0.7 \mu\text{m}^2$. The resistance minima occur only at integer flux of $\Phi = n\Phi_0$. The determination of the zero-field position again can be aided by other features such as the symmetry of the background as well as the symmetrical pair of imperfections near $\pm 7\Phi_0$.

The core reason for the profoundly different fluxoid quantization observed in GLB-A and SS-B is the slight but essential difference in the design geometries. The normal directions of the contacting crystal plane surfaces at the junctions are parallel for SS-B, where the gap function remains the same, as opposed to the antiparallel normal directions for GLB-A, where the gap functions have opposite signs. The absence of HQF in SS-B rules out alternative interpretations of the HQF observed in GLB-A. Indeed, the HQF could only originate from the odd-parity symmetry.

The Little-Parks effect in a homogeneous ring, e.g., a ring composed of a single SC, can be observed within a temperature window just below T_c . At higher temperatures, the phase coherence is lost as the SC enters the normal state, and the Little-Parks effect fades. These aspects are also present in the composite rings within the $\beta\text{-Bi}_2\text{Pd}$ segment. However, the composite rings also contain the Nb segment, which has a higher T_c . There may exist a regime where $\beta\text{-Bi}_2\text{Pd}$ loses its odd-parity characteristics but relies on the proximity effect with the contacting Nb to sustain the Little-Parks effect. In such cases, the composite ring at the elevated temperatures would behave as an even-parity singlet SC, regardless of the GLB or the SS geometry. We have indeed observed such hitherto unexplored scenarios in the GLB devices with the transition from HQF at lower temperatures to IQF at higher temperatures. Figure 3(a) shows the representative results obtained from GLB-A. The oscillations first emerge at 2.6 K with the signature of HQF. The resistance minima occur at the half-integer flux $\Phi = (n + 1/2)\Phi_0$ for 2.6 and 2.7 K. At 2.75 K, however, the HQF signature persists only for $|n| \geq 3$. For $|n| < 3$, a transitional behavior is observed. Minima may be found in both integers n or half-integers $n \pm \frac{1}{2}$. At 2.8 K, the conventional IQF is established for $|n| \leq 4$, and the transition region is pushed toward higher fields, as the oscillations for $|n| > 4$ nearly washed out. The IQF completely takes over at 2.9 K. At this point, the superconductivity in the $\beta\text{-Bi}_2\text{Pd}$ segment is dying out rapidly, and no Little-Parks effect can be observed at or above 3.0 K. In contrast, the SS-B device demonstrates only IQF throughout the temperature window (1.8–3.5 K) as shown in Fig. 3(b), with no signs of HQF.

The HQF-IQF transition has been generally observed in *all* our GLB composite rings, with additional results summarized in the Supplemental Material [17], always with the ascending temperature. The HQF and the IQF represent the Little-Parks oscillations with and without the π phase shift, respectively. The occurrence of both HQF and IQF in one device removes any doubts that the π phase shift as the signature of HQF has been correctly identified, thereby reaffirming the odd-parity symmetry in $\beta\text{-Bi}_2\text{Pd}$. Furthermore, an interesting observation can be made in GLB-A, when IQF is first developed at the low fields at 2.75 K and then pushes toward higher fields at 2.8 K.

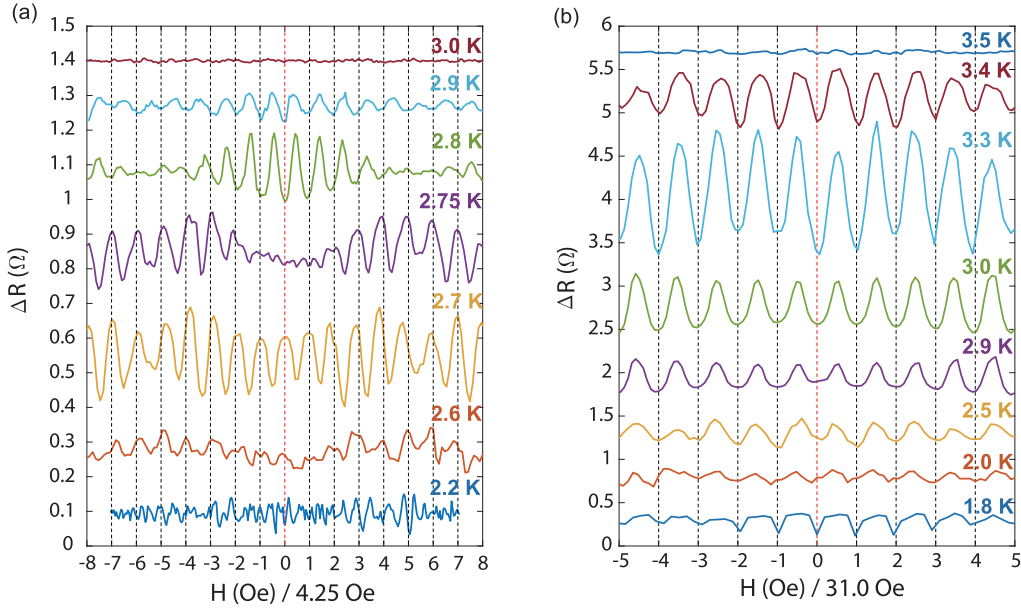


FIG. 3. Temperature dependence of the Little-Parks effect in GLB-A and SS-B rings. (a) GLB-A ($4.2 \times 1.6 \mu\text{m}^2$) with Nb connected to the opposite ends of epitaxial $\beta\text{-Bi}_2\text{Pd}$ segment demonstrates half-integer-flux quantization at 2.6 K, integer-flux quantization at 2.9 K, and a transition region in between. (b) SS-B ($1.1 \times 0.7 \mu\text{m}^2$) shows integer-flux quantization throughout. Grid lines indicate integer flux $n\Phi_0$.

It appears to suggest that a finite field helps to stabilize the triplet pairing state, while it already gives way to the even-parity singlet pairing, induced by proximity effect with Nb, near the zero field. This, at face value, is consistent with the expectation of the spin-parallel configurations of the spin-triplet states. However, this field dependence is yet to be confirmed in other GLB devices, as the transitions observed therein do not manifest sufficient fine details to resolve it.

Another intriguing question is whether the odd-parity gap structure has any angular dependence with respect to the crystalline orientations of $\beta\text{-Bi}_2\text{Pd}$. The $\beta\text{-Bi}_2\text{Pd}$ segment of GLB-A is patterned along the [100] direction of epitaxial $\beta\text{-Bi}_2\text{Pd}$. For a tetragonal lattice, it is equivalent to the [010] direction. We pattern a composite ring GLB-C with a 45° rotation, as shown in Fig. 4(a). The $\beta\text{-Bi}_2\text{Pd}$ segment is orientated along the [110] direction. Despite the new orientation, GLB-C also exhibits HQF at lower temperatures, with a transition to IQF at higher temperatures above 3 K. Applying the symmetry of the tetragonal structure, this suggests that the same odd-parity gap exists along the [110] and $[1\bar{1}0]$ directions, as well as the [100] and [010] directions. With no clear angular dependence 45° apart, the result strongly suggests that the odd-parity gap is fully open in the ab plane. Two likely p -wave configurations consistent with this observation are (a) the Anderson-Brinkman-Morel state [23] of the form $|\Delta|e^{i\phi}\sin\theta$, expressed in spherical coordinates with the z axis along the tetragonal c axis, first realized in A phase of ^3He , and (b) the Balian-Werthamer state [24], where the gap function has constant value but changes sign upon inversion as first

confirmed as the B phase of ^3He . Both configurations are symmetrically allowed for a tetragonal lattice structure [25]. On the other hand, thermodynamic property measurements of bulk $\beta\text{-Bi}_2\text{Pd}$ often conclude as fully-gapped structure [26–29], indicating the absolute value of the gap function to be a constant. The sign change in the gap function, however, cannot be detected in these measurements. Further experiments are required to fully map out the superconducting gap structure of $\beta\text{-Bi}_2\text{Pd}$.

Our previous experiment shows that HQFs can be observed in polycrystalline $\beta\text{-Bi}_2\text{Pd}$ rings [14]. A polycrystalline ring of a p -wave SC may demonstrate either HQF or IQF with about equal chances, and there are no intertransitions between the two states. For the composite rings with epitaxial $\beta\text{-Bi}_2\text{Pd}$, the only deciding factor for HQF or IQF is the device design. HQFs can be produced on demand, so long as the device geometry follows the GLB design of an epitaxial p -wave SC connected by an s -wave SC. The HQF devices, made by thin film deposition and standard lithography, are readily compatible with applications. This opens the door to applications of HQF in flux qubits [14]. For conventional flux qubits comprising only s -wave SCs, the degeneracy point must be achieved by applying a magnetic field of a precise value. Scaling up the number of flux qubits on the same chip is complicated by the requirement of a bias magnetic field. For the composite rings with the GLB design, the degeneracy is achieved at the zero magnetic field. Lifting the requirement of a bias field offers essential advantages such as better scalability, suppressed flux noise, etc. for incorporating topological

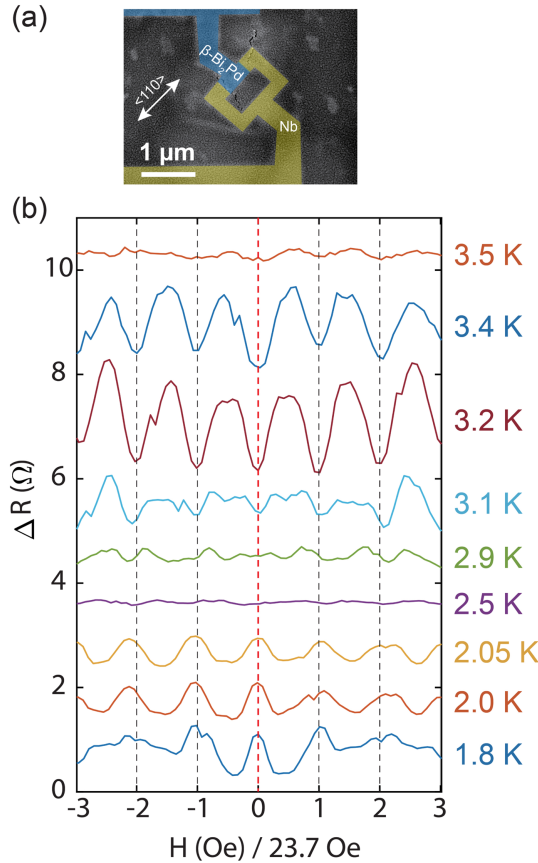


FIG. 4. Temperature dependence of the Little-Parks effect in GLB-C. (a) SEM image of composite ring device GLB-C ($1.2 \times 0.75 \mu\text{m}^2$) with Nb connected to the opposite ends of epitaxial β -Bi₂Pd segment along the $\langle 110 \rangle$ direction. (b) The Little-Parks oscillation showing the transition from half-integer-flux quantization at 2.05 K to integer-flux quantization at 3.2 K. Grid lines mark integer-flux quanta.

SCs into viable quantum information applications, a first step toward realizing the promised fault-tolerant features of topological superconductivity.

In summary, the odd-parity pairing state in β -Bi₂Pd has been unequivocally verified by HQFs observed in composite ring devices composed of epitaxial β -Bi₂Pd and s -wave SC Nb. HQF can be obtained on demand by the geometrical design of the composite ring. Transitions between HQF and IQF have been observed when the superconductivity of β -Bi₂Pd is suppressed at higher temperatures and superseded by that of the neighboring Nb. No angular dependence of the odd-parity gap has been observed along the $\langle 100 \rangle$ and $\langle 110 \rangle$ directions, implying that the gap may be isotropic in value and opposite in sign upon inversion within the ab plane. Most advantageously, a single GLB design composite ring can unequivocally reveal the even- or odd-parity nature of an unknown SC.

This work was supported by the U.S. Department of Energy, Basic Energy Science, Award Grant No. DESC0009390. Y.L. acknowledges the support by Research Grants Council, University Grants Committee of the Hong Kong SAR (Grant No. CUHK 24302822), CUHK Direct Grants (No. 4053531, No. 4053579). E-beam lithography was conducted at the University of Delaware Nanofabrication Facility (UDNF). We thank Mr. Andrew S. K. Li and the Central Laboratory of Department of Physics, CUHK for assistance in device characterization.

*Corresponding author: ustbxuxiaoying@gmail.com

Present address: Quantum Science Center of Guangdong-HongKong-Macao Greater Bay Area, Shenzhen, Guangdong, China.

†Corresponding author: yufanli@cuhk.edu.hk

‡Corresponding author: clchien@jhu.edu

- [1] D. Vollhardt and P. Wolfle, *The Superfluid Phases of Helium 3* (Taylor & Francis, London, 1990), ISBN 0850664128, 10.1201/b12808.
- [2] X.-L. Qi and S.-C. Zhang, *Rev. Mod. Phys.* **83**, 1057 (2011).
- [3] J. Alicea, *Rep. Prog. Phys.* **75**, 076501 (2012).
- [4] M. Sato and Y. Ando, *Rep. Prog. Phys.* **80**, 076501 (2017).
- [5] V. B. Geshkenbein, A. I. Larkin, and A. Barone, *Phys. Rev. B* **36**, 235 (1987).
- [6] C. C. Tsuei and J. R. Kirtley, *Rev. Mod. Phys.* **72**, 969 (2000).
- [7] M. Sigrist and T. M. Rice, *J. Phys. Soc. Jpn.* **61**, 4283 (1992).
- [8] D. A. Wollman, D. J. Van Harlingen, W. C. Lee, D. M. Ginsberg, and A. J. Leggett, *Phys. Rev. Lett.* **71**, 2134 (1993).
- [9] D. A. Wollman, D. J. Van Harlingen, J. Giapintzakis, and D. M. Ginsberg, *Phys. Rev. Lett.* **74**, 797 (1995).
- [10] K. D. Nelson, Z. Q. Mao, Y. Maeno, and Y. Liu, *Science* **306**, 1151 (2004).
- [11] A. P. Mackenzie, T. Scaffidi, C. W. Hicks, and Y. Maeno, *npj Quantum Mater.* **2**, 40 (2017).
- [12] M. Sakano, K. Okawa, M. Kanou, H. Sanjo, T. Okuda, T. Sasagawa, and K. Ishizaka, *Nat. Commun.* **6**, 8595 (2015).
- [13] Y.-F. Lv, W.-L. Wang, Y.-M. Zhang, H. Ding, W. Li, L. Wang, K. He, C.-L. Song, X.-C. Ma, and Q.-K. Xue, *Sci. Bull.* **62**, 852 (2017).
- [14] Y. Li, X. Xu, M.-H. Lee, M.-W. Chu, and C. L. Chien, *Science* **366**, 238 (2019).
- [15] X. Xu, Y. Li, and C. L. Chien, *Phys. Rev. Lett.* **124**, 167001 (2020).
- [16] Y. Li, X. Xu, S.-P. Lee, and C. L. Chien, *arXiv:2003.00603* [Phys. Rev. B (to be published)].
- [17] See Supplemental Material at <http://link.aps.org/supplemental/10.1103/PhysRevLett.132.056001> for more results and characterizations, which includes Ref. [18].
- [18] Y. Chen, *Microelectron. Eng.* **135**, 57 (2015).
- [19] W. A. Little and R. D. Parks, *Phys. Rev. Lett.* **9**, 9 (1962).

- [20] M. B. Ketchen, W. J. Gallagher, A. W. Kleinsasser, S. Murphy, and J. R. Clem, in *Proceedings of the Conference on Superconducting Quantum Interference Devices and Their Applications, SQUID '85* (De Gruyter, Berlin, 1986), pp. 865–872, <https://doi.org/10.1515/9783110862393.865>.
- [21] M. Tinkham, *Rev. Mod. Phys.* **36**, 268 (1964).
- [22] V. V. Moshchalkov, L. Gielen, C. Strunk, R. Jonckheere, X. Qiu, C. V. Haesendonck, and Y. Bruynseraede, *Nature (London)* **373**, 319 (1995).
- [23] P. W. Anderson and P. Morel, *Phys. Rev.* **123**, 1911 (1961).
- [24] R. Balian and N. R. Werthamer, *Phys. Rev.* **131**, 1553 (1963).
- [25] A. P. Mackenzie and Y. Maeno, *Rev. Mod. Phys.* **75**, 657 (2003).
- [26] E. Herrera, I. Guillamón, J. A. Galvis, A. Correa, A. Fente, R. F. Luccas, F. J. Mompean, M. García-Hernández, S. Vieira, J. P. Brison *et al.*, *Phys. Rev. B* **92**, 054507 (2015).
- [27] J. Kačmarčík, Z. Pribulová, T. Samuely, P. Szabó, V. Cambel, J. Šoltýs, E. Herrera, H. Suderow, A. Correa-Orellana, D. Prabhakaran *et al.*, *Phys. Rev. B* **93**, 144502 (2016).
- [28] P. K. Biswas, D. G. Mazzone, R. Sibille, E. Pomjakushina, K. Conder, H. Luetkens, C. Baines, J. L. Gavilano, M. Kenzelmann, A. Amato *et al.*, *Phys. Rev. B* **93**, 220504(R) (2016).
- [29] J. Chen, A. Wang, G. Pang, H. Su, Y. Chen, and H. Yuan, *Phys. Rev. B* **101**, 054514 (2020).